The 8th European Congress on Computational Methods in Applied Sciences and Engineering
ECCOMAS Congress 2022
5-–9 June 2022, Oslo, Norway

SIMULATION OF PHASE TRANSFORMATIONS IN POLYCRYSTALLINE SHAPE MEMORY ALLOYS USING FAST FOURIER TRANSFORMS

Johanna Waimann[1,2], Christian Gierden[1] AND Stefanie Reese[1]

[1] Modeling and Simulation Techniques for Systems of Polycrystalline Materials
RWTH Aachen University
Mies-van-der-Rohe-Str. 1, 52074 Aachen, Germany
e-mail: johanna.waimann@rwth-aachen.de, www.ifam.rwth-aachen.de

[2] Institute of Applied Mechanics
RWTH Aachen University
Mies-van-der-Rohe-Str. 1, 52074 Aachen, Germany
e-mail: {christian.gierden; stefanie.reese}@rwth-aachen.de, www.ifam.rwth-aachen.de

Key words: Microstructure Simulation, FFT, Shape Memory Alloys, Phase Transformation

Abstract. The properties of shape memory alloys (SMA) are mainly influenced by phase transformations between austenite and martensite. The complex material behavior is described by a variational method which describes the evolution of the phase fractions. We combined the method with a microstructural analysis based on fast Fourier transformations. Such a highly resolved microstructural analysis comes along with a high computational effort. To reduce the later one, we propose a model order reduction technique that uses just a reduced set of Fourier modes, which is adapted to the underlying microstructure. The presentation of the theoretical background as well as of the implemented algorithm is followed by numerical results that underline the performance of our method.

1 Introduction

Shape memory alloys (SMA) show a complex material behavior which is characterized by solid-solid phase transformations between austenite and martensite and parallel plastic deformations and formation of dislocations within the polycrystalline structure, see for instance [14, 23]. Compared to classical steel, not only thermal but also mechanical loads can induce this complex microstructural evolution [23]. To show the mutual effect of the microstructural evolutions and thus to predict fatigue effects of this class of smart materials, a two-scale simulation that provides a highly resolved analysis is necessary.

Besides such a highly resolved analysis of the microstructure, a multiscale simulation enables to take into account its influence on the macroscale. One possibility for the simulation of the microstructure is the use of fast Fourier transformations (FFT) based on [18, 19]. A two-scale simulation can be performed by the combination with a finite element method (FE) on the macroscale, see [22, 12]. An overview of FFT methods and their combination with FE calculations is given in [4, 17, 20].

There exist several approaches which describe the behavior of SMAs - to mention just a few of them: the probabilistic model by [5], the thermomechanical approaches by [15] and [21] as well as works which account for plastic deformations and/or functional fatigue, such as [1, 10, 16]. For the prediction of phase transformations in SMA, we use the variational method presented in [6], which is thermally coupled in [9], and extended to take into account plastic deformations in [25] as well as multiple phase transformations in steel in [26]. We combine the earlier presented variational approach with the use of FFT, which enables a localized examination of the phase transformations in the different oriented grains. Such a simulation of a highly resolved non-linear material behaviour comes along with a high computational effort. Thus, we additionally apply a model order reduction technique to reduce the computation time. The idea is to use only a reduced number of Fourier modes for the calculations in Fourier space: the considered set of Fourier modes is adapted to the underlying microstructure as presented in [3].

After a brief description of the material model in Section 2, we present the numerical method in Section 3 and proof the method's performance in Section 4 by numerical results for the microstructural analysis of nickel titanium. The paper is completed by a short summary and outlook in Section 5.

2 A variational material model for phase transformations in shape memory alloys

As mentioned in the introduction, the material behavior of shape memory alloys is dominated by a solid-solid phase transformation between austenite and martensite. Within the variational method introduced by [6], this microstructural effect is considered by a vector of volume fractions $\boldsymbol{\lambda} = \lambda_i \boldsymbol{e}_i$, including the individual fractions for austenite ($i = 0$) and n different martensitic variants ($i > 0$). Each phase is characterized by a transformation strain $\boldsymbol{\eta}_i$, a stiffness tensor $\mathbb{C}_i$ and a caloric part of the energy c_i. The inner variable $\boldsymbol{\lambda}^j$ is the phase mixture at each point within the microstructure and thus accounts for the present grain's orientation given by a set of three Euler angles $\boldsymbol{\alpha}^j$, see also Figure 1. The energy of the phase mixture at one point j within

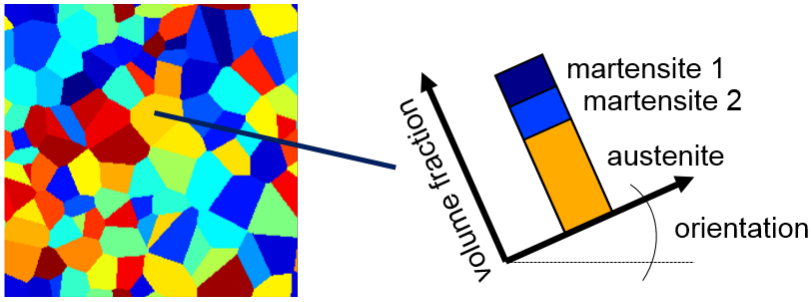

Figure 1: Concept to describe phase transformations in polycrystalline microstructure.

the microstructure is then described by the free Helmholtz energy Ψ^j:

$$\Psi^j = \frac{1}{2}\left(\boldsymbol{\varepsilon}^j - \boldsymbol{\eta}^j_{\text{eff}}\right) : \mathbb{C}^j_{\text{eff}} : \left(\boldsymbol{\varepsilon}^j - \boldsymbol{\eta}^j_{\text{eff}}\right) + c^j_{\text{eff}} \ . \tag{1}$$

In (1) the effective quantities

$$\boldsymbol{\eta}^j_{\text{eff}} = \sum_{i=0}^{n} \lambda_i^j \boldsymbol{\eta}_i^j, \qquad \mathbb{C}^j_{\text{eff}} = \left(\sum_{i=0}^{n} \lambda_i^j \left(\mathbb{C}_i^j \right)^{-1} \right)^{-1}, \qquad c^j_{\text{eff}} = \sum_{i=0}^{n} \lambda_i^j c_i \tag{2}$$

are used, whereby the stiffness tensor and the transformation strains are rotated into the grain's orientation using the rotation tensor $\boldsymbol{Q}(\boldsymbol{\alpha})$

$$\boldsymbol{\eta}_i^j = \left(\boldsymbol{Q}^j \right)^{\mathrm{T}} \cdot \boldsymbol{\eta}_i \cdot \boldsymbol{Q}^j, \qquad \mathbb{C}^j_{i,mnop} = Q^j_{qm} Q^j_{rn} Q^j_{so} Q^j_{tp} C_{i,qrst} \ . \tag{3}$$

The applied principle of the minimum of the dissipation potential is based on the idea of the minimization of a Lagrange function which consists of the rate of the Helmholtz free energy $\dot{\Psi}\left(\boldsymbol{\varepsilon}, \boldsymbol{\lambda}\right)$, a dissipation function $\mathcal{D}\left(\dot{\boldsymbol{\lambda}}\right)$ and constraints, such as the non-negativity of $\boldsymbol{\lambda}$ and the mass conservation. The minimization problem reads:

$$\mathcal{L} = \dot{\Psi}\left(\boldsymbol{\varepsilon}, \boldsymbol{\lambda}\right) + \mathcal{D}\left(\dot{\boldsymbol{\lambda}}\right) + cons \rightarrow \min_{\dot{\boldsymbol{\lambda}}} . \tag{4}$$

The dissipation function is of rate-independent type and has the form $\mathcal{D} = r|\dot{\boldsymbol{\lambda}}|$ with the so-called dissipation parameter r. The variational method is in detail described by [6] and results in the evolution equation for the volume fraction

$$\dot{\lambda}_i^j = \beta^j \operatorname{dev}_{\mathcal{A}^j} P^j_{\mathrm{T}i} \quad \forall i \in \mathcal{A}^j \tag{5}$$

with the consistency parameter β^j and the active deviator $\operatorname{dev}_{\mathcal{A}^j} P^j_{\mathrm{T}i}$. The later is calculated via

$$\operatorname{dev}_{\mathcal{A}^j} P^j_{\mathrm{T}} = P^j_{\mathrm{T}i} - \frac{1}{n^j_{\mathcal{A}}} \sum_{k \in \mathcal{A}^j} P^j_{\mathrm{T}k} \tag{6}$$

and relates the thermodynamic driving force $P^j_{\mathrm{T}i}$ of phase i at point j to the averaged driving force of the $n^j_{\mathcal{A}}$ active phases of the active set $\mathcal{A}^j = \left\{ i | \lambda_i^j > 0 \right\} \cup \left\{ i | \lambda_i^j = 0 \wedge \dot{\lambda}_i^j > 0 \right\}$. The stress tensor $\boldsymbol{\sigma}^j$ as well as $P^j_{\mathrm{T}i}$ are calculated by the partial derivatives of the energy (1)

$$\boldsymbol{\sigma}^j = \frac{\partial \Psi}{\partial \boldsymbol{\varepsilon}^j} = \mathbb{C}^j_{\text{eff}} : \left(\boldsymbol{\varepsilon}^j - \boldsymbol{\eta}^j_{\text{eff}} \right) \tag{7}$$

$$P^j_{\mathrm{T}i} = -\frac{\partial \Psi}{\partial \lambda_i^j} = \boldsymbol{\eta}^j : \boldsymbol{\sigma}^j + \frac{1}{2} \boldsymbol{\sigma}^j : \left(\mathbb{C}_i^j \right)^{-1} : \boldsymbol{\sigma}^j - c_i \ . \tag{8}$$

The consistency parameter β^j is determined by the Karush-Kuhn-Tucker conditions, which include the yield function ϕ and are also a direct result of the variational method. They read

$$\Phi^j_{\mathrm{T}} = \operatorname{dev}_{\mathcal{A}^j} \boldsymbol{P}^j_{\mathrm{T}} \cdot \operatorname{dev}_{\mathcal{A}^j} \boldsymbol{P}^j_{\mathrm{T}} - r^2 \leq 0, \qquad \beta^j \geq 0, \qquad \beta^j \Phi^j = 0 \ , \tag{9}$$

see also [6].

3 An adaptively reduced set of Fourier modes for microstructural calculations in Fourier space

In the following, the notation $\bar{(\cdot)}$ refers to quantities which are related to the macroscopic scale, such as the macroscopic strain $\bar{\boldsymbol{\varepsilon}}$. Microscopic quantities are notated without an additional sign, such as the microscopic position $\boldsymbol{x}$ and the strain tensor at the microscale $\boldsymbol{\varepsilon}$. Quantities which are related to Fourier space are given by $\hat{(\cdot)}$.

Assuming a general heterogeneous microstructure, the related boundary value problem is described by three equations: The equilibrium condition

$$\operatorname{div} \boldsymbol{\sigma}\left(\boldsymbol{x}\right) = 0 \ , \tag{10}$$

and a constitutive law for the micro stress $\boldsymbol{\sigma}(\boldsymbol{x}, \boldsymbol{\varepsilon}(\boldsymbol{x}), \boldsymbol{\lambda}(\boldsymbol{x}))$, which depends on the microscopic position, strain and the set of inner variables $\boldsymbol{\lambda}(\boldsymbol{x})$ - here the volume fractions of the martensitic variants and the austenite. The boundary value problem is completed by a description of the strain, that reads

$$\boldsymbol{\varepsilon}\left(\boldsymbol{x}\right) = \bar{\boldsymbol{\varepsilon}} + \tilde{\boldsymbol{\varepsilon}}\left(\boldsymbol{x}\right) \ . \tag{11}$$

The micro strain is thus divided in one part which is related to the macroscale $\bar{\boldsymbol{\varepsilon}}$ and one contribution $\tilde{\boldsymbol{\varepsilon}}$ that considers strain fluctuations at the microscale.

The calculation of the strain in the real space would require the solution of a convolution integral, see [13, 27], which can be hardly solved for very simple boundary value problems. We thus apply a solution strategy by [19] which performs the calculations in Fourier space. The polarization stress based on works by [7] compares the micro stress with the stress of a homogeneous reference material with a stiffness of $\mathbb{C}^0$. It has the form

$$\boldsymbol{\tau}\left(\boldsymbol{x}\right) = \boldsymbol{\sigma}\left(\boldsymbol{x}\right) - \mathbb{C}^0 : \boldsymbol{\varepsilon}\left(\boldsymbol{x}\right) \ . \tag{12}$$

After the transformation of $\boldsymbol{\tau}$ into Fourier space and hence receiving $\hat{\boldsymbol{\tau}}$, one can calculate the strain in Fourier space

$$\hat{\boldsymbol{\varepsilon}}(\boldsymbol{\xi}) \ = \ \begin{cases} -\hat{\boldsymbol{\Gamma}}^0(\boldsymbol{\xi}) \ : \ \hat{\boldsymbol{\tau}}(\boldsymbol{\xi}) & \text{for } \boldsymbol{\xi} \ \neq \ \mathbf{0} \\ \ \bar{\boldsymbol{\varepsilon}} & \text{for } \boldsymbol{\xi} \ = \ \mathbf{0} \end{cases} \ . \tag{13}$$

The Lippmann-Schwinger equation (13) depends on the Greens function and operator in Fourier space

$$\hat{\Gamma}^0_{ijkl}(\boldsymbol{\xi}) = \frac{1}{2}\left(\hat{G}^0_{ik}(\boldsymbol{\xi})\xi_j\xi_l \ + \ \hat{G}^0_{jk}(\boldsymbol{\xi})\xi_i\xi_l\right) \quad \hat{G}^0_{ik}(\boldsymbol{\xi}) = (\mathbb{C}^0_{ijkl}\xi_j\xi_l)^{-1} \tag{14}$$

and a set of Fourier modes $\boldsymbol{\xi}$.

To reduce the computational effort of solving the Lippmann-Schwinger equation, a reduced set of Fourier modes may be considered, while the quality of the reached solution highly depends on the set of chosen modes: either on the number as well as on the specific choice, see [2, 11]. Based on our previous work in [3], we adaptively choose the reduced set of modes ${}^R\boldsymbol{\xi}^i$ by taking

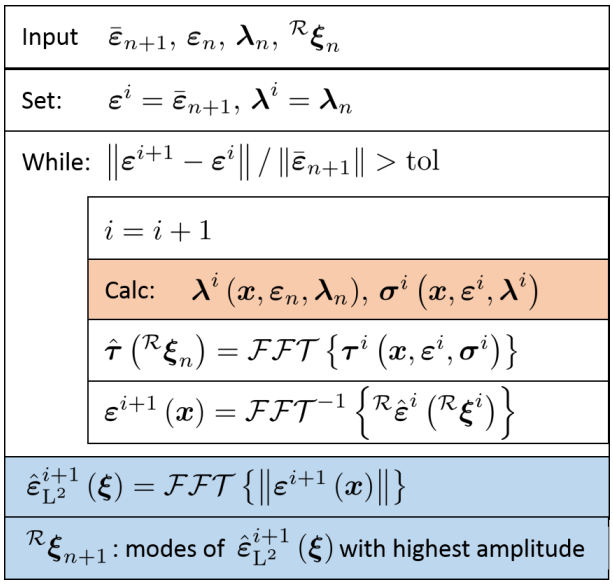

Figure 2: Algorithm to describe phase transformations in polycrystalline microstructure.

into account the current strain field $\boldsymbol{\varepsilon}^i$ of the observed boundary value problem. The algorithm is also presented in Figure 2: For the current load step $n+1$, we prescribe the macroscopic strain tensor $\bar{\boldsymbol{\varepsilon}}_{n+1}$. In addition, the microscopic strain field as well as the inner variables and the reduced set of Fourier modes are known from the former load step n. The current micro strain is iterativeley calculated using the basic fixed point scheme. For each iteration step i, the volume fractions and the stress are calculated based on the material model given in Section 2 (*orange*). They then influence the polarization stress $\boldsymbol{\tau}$ and with that the strain tensor. When the latter one converges, its L2-norm is transformed into Fourier's space using the full set of modes. Then, the frequencies with the highest amplitudes are identified and used for the following load step (*blue*). The percentage of chosen modes is given by $\mathcal{R}$. Further information about the model order reduction technique can be found in [3].

4 Numerical results

For the numerical results, we assume nickel titanium (NiTi) and thus a transformation between austenite and twelve different martensitic variants. The elastic constants $\mathbb{C}_i$ as well as the transformation strains are taken from [24, 8]. The dissipation parameter is assumed with 0.006 GPa and the caloric energies with $c_0 = -0.03$ GPa and $c_{i>0} = 0.0$ GPa. The calculations are performed using a microstructure discretized by 127×127 grid points and $\mathcal{R} = 1\%$ of Fourier modes.

The stepwise prescription of a tensile strain $\varepsilon_{\mathrm{xx}} = 0.04\,[\text{-}]$ results in the macroscopic stress-strain relation given in Figure 3. The classical hysteresis curve is characteristic for the pseudoelastic behavior of SMA: First, the originally austenitic material behaves linear elastic. After reaching a certain stress, the transformation from austenite to martensite takes place resulting in a stress plateau. The smooth transition in Figure 3 stems from the different starting points in

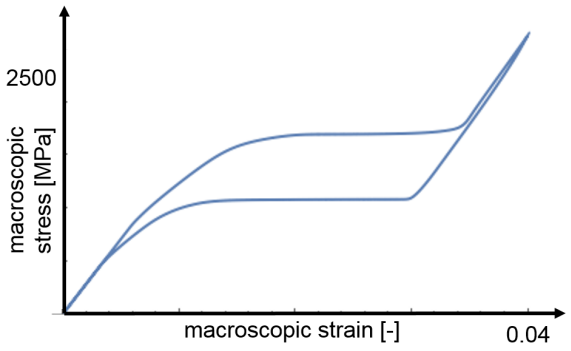

Figure 3: Macroscopic stress-strain relation.

the individual grains. When the transformation is finished, the stress increases again. Unloading then leads to a back transformation into austenite and with that to a second stress plateau, which is smaller than the first one. When the reverse transformation is completed, the material again behaves linear elastic.

Figure 4 shows the microstructural evolution of the strain as well as the austenitic volume fraction within the assumed polycrystal. In the beginning, the isotropic austenite results in a homogenous strain state. During the transformation, higher strain concentrations at the grain's boundaries are accompanied with a there initiated transformation into martensite. When the transformation is completed, the anisotropic polycrystalline structure consisting of different martensitic variants leads to the still visible strain concentrations at the grain boundaries.

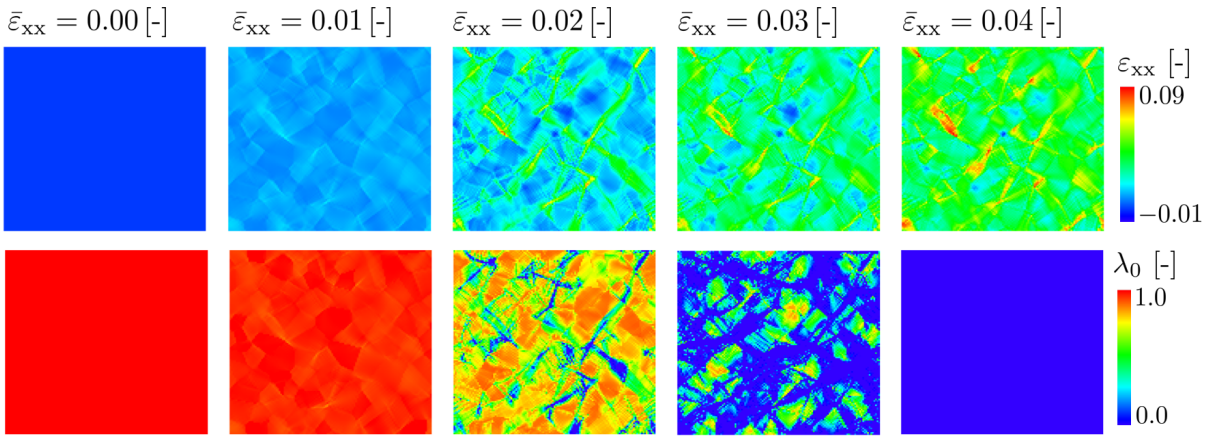

Figure 4: Microstructural evolution of the strain ε_{xx} (top) and the austenitic volume fraction λ_0 (bottom) for different macroscopic strains $\bar{\varepsilon}_{xx}$ for the loading path.

In Figure 5, the absolute microscopic error in the strain field $\Delta\varepsilon_{xx} = |\varepsilon_{xx}^{100\%} - \varepsilon_{xx}^{1\%}|$ (*left*)

as well as the relative macroscopic error in the stress field $\Delta\bar{\sigma}_{\mathrm{xx}} = (\bar{\sigma}_{\mathrm{xx}}^{\mathcal{R}\%} - \bar{\sigma}_{\mathrm{xx}}^{100\%})/\bar{\sigma}_{\mathrm{xx}}^{100\%}$ (*left*) are presented. Both errors compare the solution with the reduced number of Fourier modes with the unreduced calculation. The microscopic error is given for a prescribed macro strain of $\bar{\varepsilon}_{\mathrm{xx}} = 0.03\,[\text{-}]$ and shows just small differences of a solution with $\mathcal{R} = 1\,\%$ compared to the reference solution. The macroscopic error is given for the loading path ($\dot{\bar{\varepsilon}} > 0$) and is also small. It mainly appears for the start and the end of the transformation.

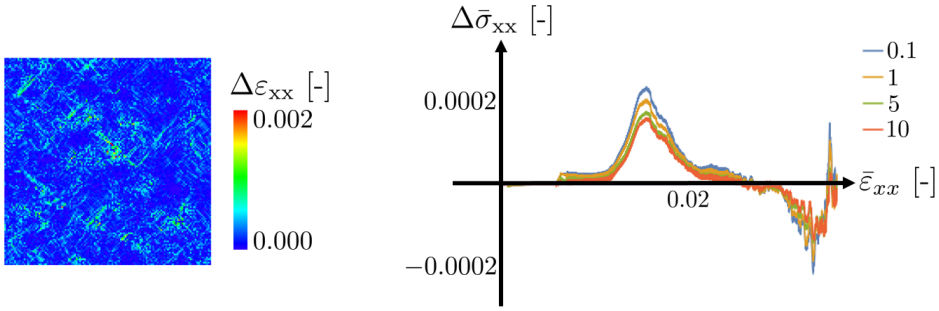

Figure 5: Errors of the reduced solution with $\mathcal{R} = 1\%$ of Fourier modes compared to the unreduced calculation: microscopic error of the strain $\Delta\bar{\varepsilon}_{\mathrm{xx}}$ for $\bar{\varepsilon}_{\mathrm{xx}} = 0.03\,[\text{-}]$ (*left*), macroscopic error of the stress $\Delta\bar{\sigma}_{\mathrm{xx}}$ for the loading path (*right*).

5 Conclusions

We presented the application of a model order reduction technique for calculations using Fast Fourier Transformations for the microstructural analysis of phase transformations in polycrystalline shape memory alloys. For the consideration of the transformations between austenite and martensite, we used the variational method introduced by [6]. By the presentation of numerical results, we were able to show the pseudoelastic behavior of the polycrystal considering the highly resolved microstructure. The model order reduction technique is based on the idea of an adaptively chosen reduced set of Fourier modes by [3]. The set is determined based on the microstructural strain field of the former load step and guarantees a reduction of the numerical effort without producing high errors.

In our future works, we will implement the developed algorithm into a two sale approach in which we will perform a finite element analysis for the macroscale. Additionally, we want to couple the phase transformations with other microstructural effects, such as crystal plasticity, to examine the fatigue behavior of SMAs.

Acknowledgements. The authors gratefully acknowledge the financial support of the research work by the German Research Foundation (DFG, Deutsche Forschungsgemeinschaft) within the transregional Collaborative Research Center SFB/TRR 136, project number 223500200, subprojects M03 and M05.

REFERENCES

[1] Bartel, T., Osman, M. and Menzel, A. A phenomenological model for the simulation of functional fatigue in shape memory alloy wires. *Meccanica* (2016), 1–16.

[2] Gierden, C., Waimann, J., Svendsen, B. and Reese, S. A geometrically adapted reduced set of frequencies for a FFT-based microstructure simulation. *Comput. Methods Appl. Mech. Eng.* (2021) **386**:114131.

[3] Gierden, C., Waimann, J., Svendsen, B. and Reese, S. FFT-based simulation using a reduced set of frequencies adapted to the underlying microstructure. *Comput. Methods Mater. Sci.* (2021) **21**(1):51–58.

[4] Gierden, C., Kochmann, J., Waimann, J., Svendsen, B. and Reese, S. A review of FE-FFT-based two-scale methods for computational modeling of microstructure evolution and macroscopic material behavior. *Arch. Computat. Methods Eng.* (2022), 1–21.

[5] Govindjee, S. and Hall, G.J. A computational model for shape memory alloys. *Int. J. Solids Struct.* (2000), **37**(5):735–760.

[6] Hackl, K. and Heinen, R. A micromechanical model for pretextured polycrystalline shape-memory alloys including elastic anisotropy. *Continuum Mech. Thermodyn.* (2008) **19**(8):499–510.

[7] Hashin, Z. and Shtrikman, S. On some variational principles in anisotropic and nonhomogeneous elasticity. *J. Mech. Phys. Solids* (1962) **10**(4):335–342.

[8] Junker, P. *Simulation of shape memory alloys: material modeling using the principle of maximum dissipation.* Inst. Mech. Schriftenreihe (2011).

[9] Junker, P. and Hackl, K. A thermo-mechanically coupled field model for shape memory alloys. *Contin. Mech. Thermodyn.* (2014) **26**(6):859–877.

[10] Junker, P. and Hempel, P. Numerical Study of the Plasticity-Induced Stabilization Effect on Martensitic Transformations in Shape Memory Alloys. *Shape Memory and Superelasticity* (2017) **3**(4):422–430

[11] Kochmann, J., Manjunatha, K., Gierden, C., Wulfinghoff, S., Svendsen, B. and Reese, S. A simple and flexible model order reduction method for FFT-based homogenization problems using a sparse sampling technique. *Comput. Methods Appl. Mech. Eng.* (2019) **347**:622–638.

[12] Kochmann, J., Wulfinghoff, S., Reese, S., Mianroodi, J. R. and Svendsen, B. Two-scale FE–FFT-and phase-field-based computational modeling of bulk microstructural evolution and macroscopic material behavior. *Comput. Methods Appl. Mech. Eng.* (2016) **305**:89–110.

[13] Kröner, E. Allgemeine Kontinuumstheorie der Versetzungen und Eigenspannungen. *Arch. Ration. Mech. Anal.* (1959) **4**(1):273–334.

[14] Krooss, P., Ninendorf, T., Kadletz, P. M., Somsen, C., Gutmann, M. J., Chumlyakov, Y. I., Schmahl, W. W., Eggeler, G. and Maier, H. J. Functional Fatigue and Tension–Compression Asymmetry in [001]-Oriented Co49Ni21Ga30 High-Temperature Shape Memory Alloy Single Crystals. *Shape Mem. Superelasticity* (2015) **1**(1):6–17.

[15] Lagoudas, D. C. *Shape memory alloys: modeling and engineering applications.* Springer, (2008).

[16] Xu, L., Solomou, A., Baxevanis, T. and Lagoudas, D. Finite strain constitutive modeling for shape memory alloys considering transformation-induced plasticity and two-way shape memory effect. *Int. J. Solids Struct.* (2021), **221**:42–59.

[17] Lucarini, S., Upadhyay, M.V. and Segurado, J. FFT based approaches in micromechanics: fundamentals, methods and applications. *Model. Simul. Mater. Sci. Eng.* (2021) **30**:023002.

[18] Moulinec, H. and Suquet, P. A fast numerical method for computing the linear and nonlinear mechanical properties of composites. *C. R. Acad. Sci., S´erie II b* (1994) **318**(11):1417–1423.

[19] Moulinec, H. and Suquet, P. A numerical method for computing the overall response of nonlinear composites with complex microstructure. *Comput. Methods Appl. Mech. Eng.,* (1998) **157**(1-2):69–94.

[20] Schneider, M. A review of nonlinear FFT-based computational homogenization methods. *Acta Mech.* (2021) **232**:2051–2100.

[21] Frost, M., Benešová, B., Seiner, H. and Kružík, M., Šittner, P. and Sedlák, P. Thermomechanical model for NiTi-based shape memory alloys covering macroscopic localization of martensitic transformation. *Int. J. Solids Struct.* (2021) **221**:117–129.

[22] Spahn, J., Andrä, H., Kabel, M. and Müller, R. A multiscale approach for modeling progressive damage of composite materials using fast Fourier transforms. *Comput. Methods Appl. Mech. Eng.* (2014) **268**:871–883.

[23] Wagner, M. F.-X. *Ein Beitrag zur strukturellen und funktionalen Ermudung von Draehten und Federn aus NiTi-Formgedaechtnislegierungen.* Europ. Univ.-Verlag (2005).

[24] Wagner, M. F.-X. and Windl, W. Lattice stability, elastic constants and macro- scopic moduli of NiTi martensites from first principles. *Acta Mater.* (2008) **56**(20):6232–6245.

[25] Waimann, J., Junker, P. and Hackl, K. Modeling the cyclic behaviour of shape memory alloys. *Shap. Mem. Superelasticity* (2017) **3**:124–138.

[26] Waimann, J. and Reese, S. Variational modeling of temperature induced and cooling-rate dependent phase transformations in polycrystalline steel. *Mech. Mater.* (2002) **170**:104229.

[27] Willis, J. R. Variational and related methods for the overall properties of composites. *Advances in applied mechanics* (1981) **21**:1–78.